JOURNAL OF Materials CHEMISTRY

Plasma polymerization of allylpentafluorobenzene on copper surfaces

G. H. Yang,[a] Yan Zhang,[a] E. T. Kang,*[a] K. G. Neoh,[a] A. C. H. Huan[b] and D. M. Y. Lai[b]

[a]*Department of Chemical Engineering, National University of Singapore, Kent Ridge, Singapore 119260. E-mail: cheket@nus.edu.sg; Fax: (65) 779-1936*
[b]*Institute of Materials Research and Engineering (IMRE), National University of Singapore, 3 Research Link, Singapore 117602*

Received 1st October 2001, Accepted 16th November 2001
First published as an Advance Article on the web 31st January 2002

Fluoropolymer films were deposited on pristine and N_2 plasma-pretreated copper foil surfaces by plasma polymerization of allylpentafluorobenzene (APFB) under different glow discharge conditions and using argon as the carrier gas. The effect of the radio-frequency (RF) plasma power on the surface composition and chemical structure of the plasma-polymerized APFB (pp-APFB) films was studied by X-ray photoelectron spectroscopy (XPS), Fourier transform infrared (FTIR) spectroscopy, time-of-flight secondary ion mass spectrometry (ToF-SIMS) and water contact angle measurements. The XPS, ToF-SIMS and FTIR results suggested that the fluorinated aromatic structure in the deposited polymer films had been preserved to various extents, depending on the input RF power used for the plasma polymerization. The roughness of the APFB plasma-polymerized copper (pp-APFB-Cu) surface increased substantially with the RF power, as revealed by atomic force microscopy (AFM) and scanning electron microscopy (SEM). Ultra-hydrophobic pp-APFB-Cu surfaces with water contact angles greater than 140° were obtained at RF powers above 50 W. The solvent extraction and the Scotch® tape peel test results revealed that the pp-APFB layers were strongly bonded to the N_2 plasma-pretreated copper surfaces.

1. Introduction

With the continuous decrease in integrated circuit dimensions, significant reductions in both resistance and capacitance of the interconnects are needed in the development of ultra large-scale integrated circuits (ULSI).[1] To reduce the resistance of the metal interconnects, copper has been proposed as an alternative metal to aluminium. The lower resistivity of copper lines can effectively reduce interconnect delays. Copper also has a higher melting point and higher resistance to electromigration and stress-induced voiding.[2,3] On the other hand, to reduce the capacitance of the interlayer dielectrics, new materials with lower dielectric constants than conventional silicon dioxide are needed.[1] A number of studies involving copper metallization on low dielectric constant materials of importance to the microelectronic industry have been reported recently.[4,5]

Fluoropolymers are promising materials for dielectric applications due to their low dielectric constants and high thermal stability.[6] Their application in microelectronics, however, has been hindered by the difficulty in processing.[7] The traditional processing methods for microelectronic applications, such as spin and solution coating, are generally not applicable to fluoropolymers. Plasma polymerization provides an alternative approach to overcoming the processing problem. It is a convenient way to deposit fluoropolymer films of controlled thickness and properties in the absence of a solvent.[8–11] Furthermore, it is a rapid, simple and low temperature process.[12] A number of studies[13–20] on plasma polymerization of fluoromonomers have been carried out to produce fluoropolymer films with ultra-hydrophobic properties and low dielectric constants. On the other hand, deposition of fluoropolymers on copper substrates by plasma polymerization, the interaction between the plasma-deposited fluoropolymer and the substrate, and the preservation of the molecular structure in the resulting fluoropolymer films have yet to be studied in detail.

In the present work, 1-allylpentafluorobenzene (APFB) polymer thin films are deposited directly on the copper foil surfaces by RF plasma polymerization of the APFB monomer. The choice of the monomer is based on the following justifications. The high reactivity of the allyl group and the relative stability of the aromatic group in APFB are expected to give rise to a plasma polymer having a similar chain structure and fluorine content to those of the APFB homopolymer. The chemical composition and structure of the plasma polymerized APFB (pp-APFB) films are investigated by X-ray photoelectron spectroscopy (XPS), time-of-flight secondary mass spectrometry (ToF-SIMS), and Fourier transform infrared (FTIR) spectroscopy. The hydrophobility of the pp-APFB films is studied by water contact angle measurements. The surface morphologies of the pp-APFB films, on the other hand, are studied by atomic force microscopy (AFM) and scanning electron microscopy (SEM).

2. Experimental

2.1 Materials

Copper foil (99.9% purity) having a thickness of about 0.1 mm, was purchased from Goodfellow Ltd. of Cambridge, UK. The surface of the foil was cleaned with 0.1 M HCl solution for 10 min, followed by rinsing with doubly-distilled water. The 1-allylpentafluorobenzene (APFB) monomer used for plasma polymerization was obtained from the Aldrich Chemical Company of Milwaukee, WI, USA. The chemical structure of APFB is shown below:

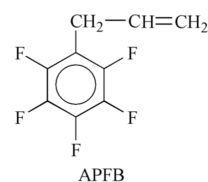

 DOI: 10.1039/b108895p

This journal is © The Royal Society of Chemistry 2002

2.2 Plasma polymerization of APFB

Plasma polymerization of APFB was carried out on an apparatus manufactured by Samco International of Kyoto, Japan (Model Samco BP-1). The physical geometry of the apparatus has been described previously.[21,22] An RF generator provided power supplies from 0 to 200 W and was operated at a frequency of 13.56 MHz. Plasma polymerization and deposition processes were performed between two circular parallel plate electrodes. The copper substrates were placed on the ground electrode, which was about 2.8 cm away from the biased electrode. At a specific temperature, the APFB monomer was introduced into the deposition chamber by the argon carrier gas flowing through a thermostated monomer reservoir. All the gas lines were electrically heated to a temperature slightly higher than that of the monomer reservoir by means of band heaters. The monomer–carrier gas mixture was allowed to flow evenly into the reactor from a distributor located in the upper electrode. In all cases, the carrier gas stream was assumed to be saturated with the APFB monomer, as dictated by the partial pressure of the latter. The glow discharge was ignited, after impedance matching, at a system pressure of 100 Pa, an Ar flow rate of 20 standard cubic centimetres per min (sccm), and a monomer temperature of 25 °C. Each time, the glow discharge was maintained for 40 s to allow the deposition of a film of 1 to 3 μm in thickness, depending on the RF power used.

2.3 Surface characterization

XPS measurements were made on a Kratos AXIS HSi spectrometer (Kratos Analytical Ltd., England) with a monochromatized Al K_α X-ray source (1456.6 eV photons) at a constant dwell time of 100 ms, and pass energy of 40 eV. The anode voltage was 15 kV. The anode current was 10 mA. The pressure in the analysis chamber was maintained at 5.0×10^{-8} Torr or lower during each measurement. The surface-modified Cu foils were mounted on the standard sample stubs by means of double-sided adhesive tapes. The core-level signals were obtained at a photoelectron take-off angle of 90° (with respect to the sample surface). All binding energies (BE's) were referenced to the C 1s hydrocarbon peak at 284.6 eV. In peak synthesis, the line width (full width at half maximum or FWHM) of the Gaussian peaks was maintained constant for all components in a particular spectrum. Surface elemental stoichiometries were determined from peak-area ratios, after correcting with the experimentally determined sensitivity factors, and were reliable to ±10%. The elemental sensitivity factors were determined using stable binary compounds of well-established stoichiometries.

Time-of-flight secondary ion mass spectrometry (ToF-SIMS) was also employed for the surface analysis of the pp-APFB films on copper substrates. The ToF-SIMS analysis was carried out on an ION-TOF SIMS IV instrument (ION-TOF, GMBH, Germany). The primary ion beam (10 keV Ar^+) with a spot size of ~50 μm was rastered over an area of $500 \times 500\ \mu m^2$ while keeping the total dose under 10^{13} ions cm^{-2}. The pressure in the analysis chamber was maintained at 1×10^{-9} Torr or lower during each measurement. To reduce the charging effect, an electron flood gun was used for the charge neutralization. The calibration of the mass spectra was based on the built-in mass library.

The morphology of the pristine and surface-modified copper foils was characterized using a Nanoscope IIIa atomic force microscope (AFM). All images were obtained in the air using the tapping mode under a constant force (scan size: 5 μm × 5 μm, set point: 3.34 μV, scan rate: 1.0 Hz). Scanning electron microscopy (SEM) images of the pristine copper foil and the pp-APFB-Cu surfaces were obtained on the JEOL, JSM 5600LV, scanning electron microscope.

2.4 FTIR spectra

The pp-APFB samples for Fourier transform infrared (FTIR) spectroscopy measurements were obtained by direct plasma polymerization and deposition of APFB on the freshly pressed KBr pellets at a system pressure of 100 Pa, an Ar flow rate of 20 sccm, and a monomer temperature of 25 °C for about 5 min. The FTIR spectra were recorded in air on a Bio-Rad FT-IR, Model 400, spectrophotometer. Each spectrum was collected by accumulating 30 scans at a resolution of 8 cm^{-1}.

2.5 Water contact angle measurements

The static water contact angles were measured at 25 °C and 65% relative humidity on a telescopic goniometer (Rame–Hart model 100-00(230)). The telescope, with a magnification power of 23×, is equipped with a protractor of 1° graduation. For each angle reported, at least five readings from different surface locations were averaged.

The angles reported were reliable to ±3°.

3. Results and discussion

3.1 Composition of the plasma polymerized APFB films on copper foil surfaces

Figs. 1(a) to 1(c) show the C 1s core-level spectra of the plasma polymerized APFB on copper foil surfaces (pp-APFB-Cu surfaces) prepared at the input RF powers of 5 W (Fig. 1(a)), 35 W (Fig. 1(b)), and 80 W (Fig. 1(c)). The C 1s core-level spectra can be curve-fitted with peak components having binding energies (BE's) at 284.6 eV for the C–H species, at 285.2 eV for the C–CF species, at 287.2 eV for the CF (aromatic) species, and at 289.8 eV for the CF_2CH_2 species.[23] In addition, the broad high binding energy peak at 293.2 eV is assigned to the π–π* shake-up satellite associated with the aromatic ring of the APFB unit.[14,24]

It is obvious that the input RF power can greatly influence the chemical composition of the plasma polymerized APFB (pp-APFB) film on the copper surface. The relative intensity of the aromatic CF species decreases with increasing RF power. On the other hand, the relative intensity of the CF_2CH_2 species, formed during the plasma polymerization process, increases with increasing RF power. The theoretical ratio for the [CH]: [C–CF]: [CF] species in the APFB homopolymer is 3 : 1 : 5. For

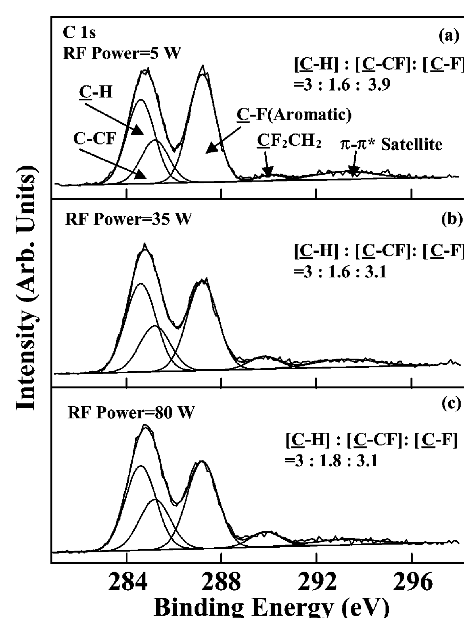

Fig. 1 C 1s core-level spectra of the plasma polymerized APFB on copper foil surfaces at RF powers of (a) 5 W, (b) 35 W, and (c) 80 W.

the pp-APFB film deposited at the low RF power of 5 W, this ratio is 3 : 1.6 : 3.9. On the other hand, for the pp-APFB films deposited at the higher powers of 35 W and 80 W, the corresponding ratios are 3 : 1.6 : 3.1, and 3 : 1.8 : 3.1, respectively. Thus, the fluorinated aromatic rings in the pp-APFB film are preserved more effectively for deposition carried out at the low RF power of 5 W.

The variation in composition of the pp-APFB film with the RF power probably arises from the difference in bond scission mechanism during the plasma polymerization process. Taking into account the *W*/*FM* parameter,[25] where *W*, *F*, and *M* are the input RF power, the monomer flow rate, and the molecule weight of the monomer, respectively, plasma polymerization proceeds in the energy-deficient state at the low RF power of 5 W. The energy per unit mass of the molecule is low. Bond scission occurs mainly at the π-bond of the allyl group, which has the lowest bond energy[26,27] in the APFB molecule. Under these conditions, rearrangement of the active radicals results in a plasma polymer having a similar chain structure to that of the APFB homopolymer. As the RF power is increased, the plasma polymerization process transforms from an energy-deficient state to a more energetic state. More energy per unit mass of the monomer is available at the higher RF power, leading to more severe molecular fragmentation. Under these conditions, the APFB plasma has more active radicals, which come from scissions of the π-bond of the allyl group, as well as scissions of the C–H and the C–F bonds. The latter reactions help to account for the decrease in intensity of the <u>C</u>–F component and the formation of more <u>C</u>F_2CH_2 species in the pp-APFB film with increasing RF power.

3.2 Chemical structure of the pp-APFB Films

The ToF-SIMS spectra of the pp-APFB films deposited on copper surfaces at different input RF powers of 5 W and 80 W are shown in Fig. 2(a) and Fig. 2(b), respectively. The assignments of the positive ions of the pp-APFB films are shown in Scheme 1 below. The preservation of the fluorinated aromatic ring is indicated by the strong C_6F_5-CH_2 peak (peak A in Fig. 2) intensity observed and the presence of the APFB repeat units. It can be observed that the relative peak intensities of the C_6F_5-CH_2 species and the APFB repeat units for the pp-APFB film deposited at a RF power of 5 W are much higher than those of the corresponding species for the pp-APFB film deposited at a RF power of 80 W. On the other hand, the relative intensity of the C_6F_5 (peak B in Fig. 2) species is higher for the pp-APFB film deposited at a higher RF power of 80 W.

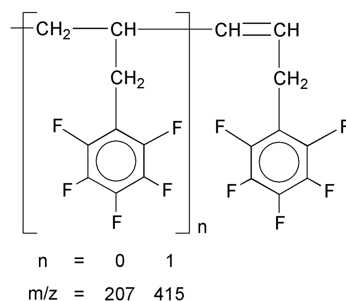

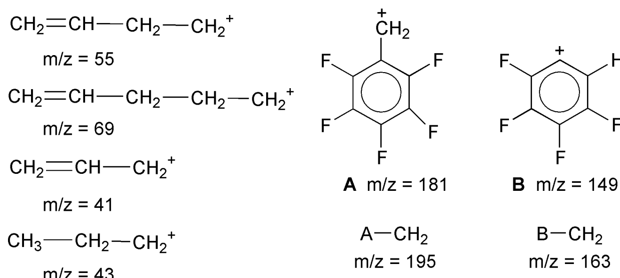

Scheme 1 Assignment of positive ions in ToF-SIMS.

Fig. 3 shows the respective FTIR spectra of the APFB monomer (Fig. 3(a)) and the pp-APFB films deposited on KBr pellets at RF powers of 5 W (Fig. 3(b)) and 80 W (Fig. 3(c)). The FTIR spectrum of the APFB monomer displays the

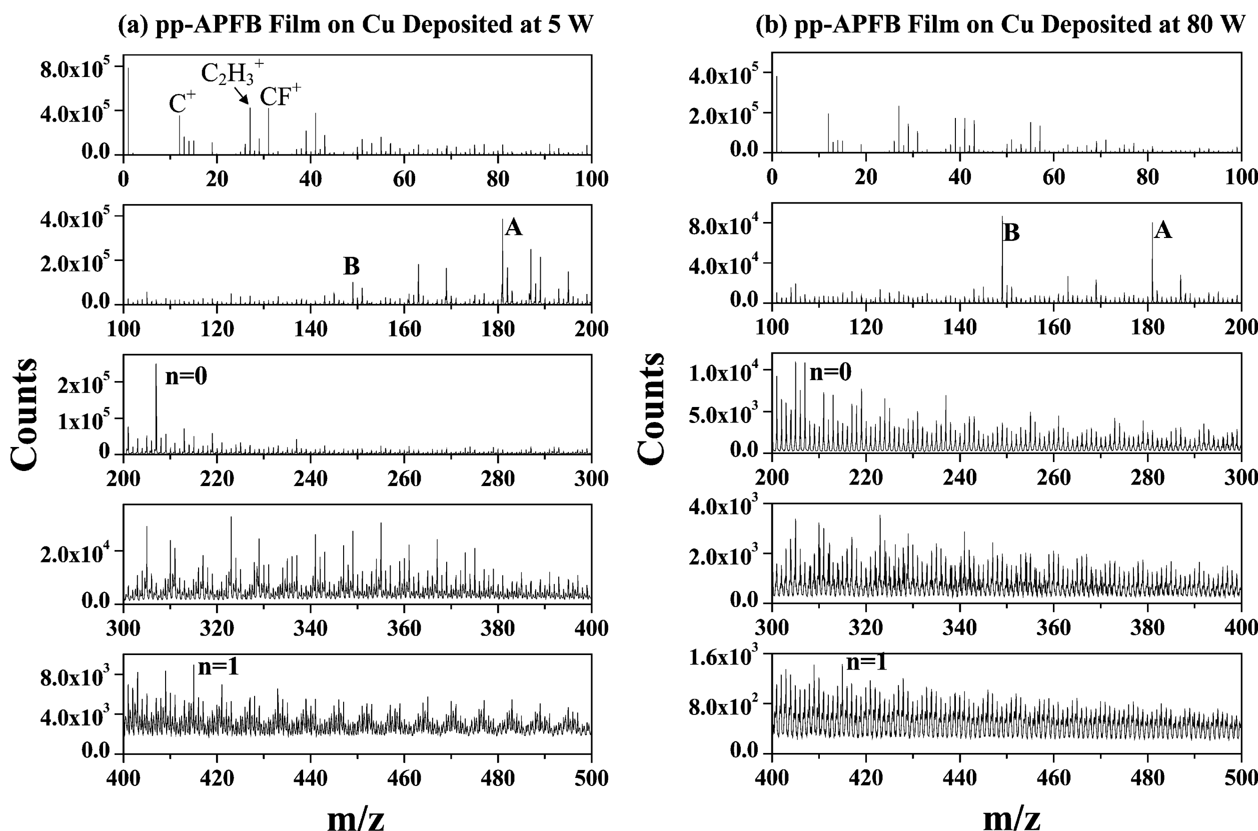

Fig. 2 Positive ion ToF-SIMS spectra of the pp-APFB films on copper foil deposited at RF powers of (a) 5 W and (b) 80 W.

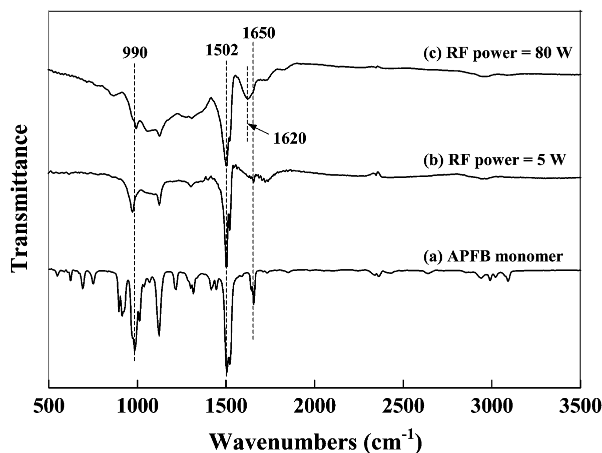

Fig. 3 FTIR spectra of (a) the APFB monomer, and the plasma polymerized APFB (pp-APFB) films on KBr discs at RF powers of (b) 5 W and (c) 80 W.

characteristic absorption bands of the aromatic C–F species at a wavenumber of 990 cm^{-1} and of the fluorinated aromatic rings at a wavenumber of 1502 cm^{-1}.[14] The absorption band at a wavenumber of 1650 cm^{-1} is assigned to the stretching absorption of the allyl C=C species.[14] Thus, it can be observed that the characteristic absorption band at 990 cm^{-1} for the aromatic C–F species has been preserved to a large extent for the pp-APFB films deposited at 5 W (Fig. 3(b)). On the other hand, however, the intensity of the corresponding absorption band for the film deposited at 80 W has decreased substantially (Fig. 3(c)). The presence of aromatic rings with a reduced degree of fluorination is also indicated by the appearance of the absorption band[28] at about 1620 cm^{-1} in Figs. 3(c). The enhanced absorption at wavenumbers of 1100–1300 cm^{-1} in Fig. 3(c), on the other hand, is due to the overlapping absorption of the CF_x species (x = 1–3).[29] The presence of CF_x species in the pp-APFB films is consistent with the XPS results in Fig. 1. The FTIR results also suggest that the plasma polymerization of APFB has proceeded mainly through the allyl C=C bonds, as indicated by the almost complete loss of the allyl C=C absorption at 1650 cm^{-1} for the pp-APFB films.

3.3 Morphology of the pp-APFB-Cu surfaces

There are significant differences in surface morphology among the pp-APFB films deposited under various conditions. Fig. 4 shows the respective AFM (left-hand side) and SEM (right-hand side) images of the pristine copper surface (Fig. 4(a)), and the pp-APFB-Cu surfaces prepared at input RF powers of 5 W (Fig. 4(b)) and 80 W (Fig. 4(c)). The pristine copper foil surface used in this work has an average surface roughness value (R_a) of about 23 nm. The pp-APFB film prepared at a low RF power of 5 W has a smoother surface. The R_a value is only about 2.1 nm. The smooth morphology suggests that the plasma polymerization has occurred predominantly on the substrate surface, instead of in the gas phase.[16] This polymerization mechanism at low RF power results in a lower deposition rate (in comparison to the deposition rate at high RF power, see below) of about 280 Å s^{-1}, as measured on Si(100) surface using an Alpha-STEP 500 Surface Profiler. The pp-APFB-Cu surface prepared at a RF power of 80 W, on the other hand, has a relatively rough surface with an R_a value of about 102 nm, suggesting that the plasma polymerization has occurred mainly in the gas phase. The particles are formed in the gas phase and then deposited on the substrate (SEM image in Fig. 4(c)). Under these conditions, the deposition rate, as measured on the Si(100) substrate surface, is higher than 600 Å s^{-1}.

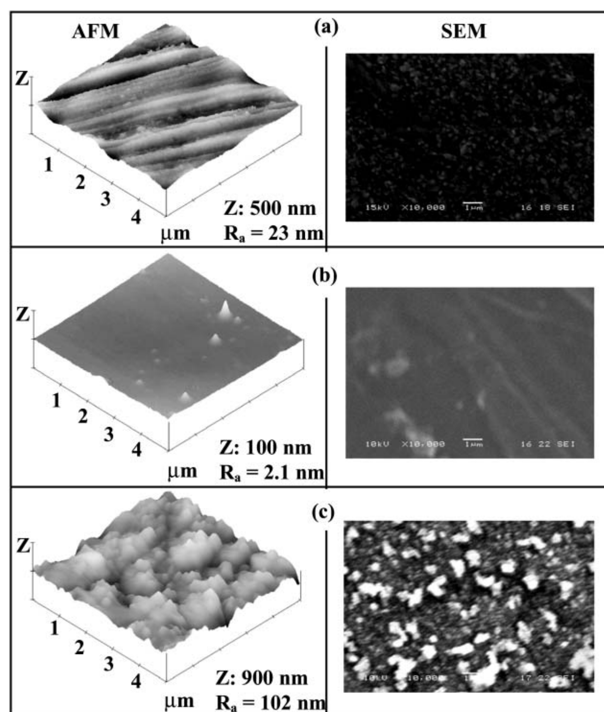

Fig. 4 AFM and SEM images of (a) the pristine Cu surface and the pp-APFB-Cu surfaces obtained at RF powers of (b) 5 W and (c) 80 W.

3.4 Water contact angles of the pp-APFB-Cu surfaces

The pp-APFB-Cu surface is expected to exhibit a considerable degree of hydrophobicity. Fig. 5 shows the dependence of the surface roughness (R_a), as calculated from the roughness profile determined by AFM, and the water contact angle of the pp-APFB-Cu surface on the input RF power used for the plasma polymerization. The [F]/[C] ratio for the starting APFB monomer is 0.56. The [F]/[C] ratios of the deposited pp-APFB films are slightly lower. However, the ratio varies only from about 0.49 to about 0.44 when the RF power is increased from 5 W to 80 W. Thus, defluorination has occurred only to a limited extent, even at a high input RF power of 80 W. The minor variation in the [F]/[C] ratio cannot account for the large increase in the observed water contact angle. On the other hand, the increase in water contact angle with the RF power coincides approximately with the increase in the surface roughness value. The surface roughness and the static contact angle can be related by the equation proposed by Good:[30]

$$\cos \theta_r = r \cos \theta_{true}$$

where θ_r, θ_{true} and r are the apparent static contact angle with a solid surface, the true static angle with a geometrically 'smooth' surface, and the roughness factor of the surface, respectively.

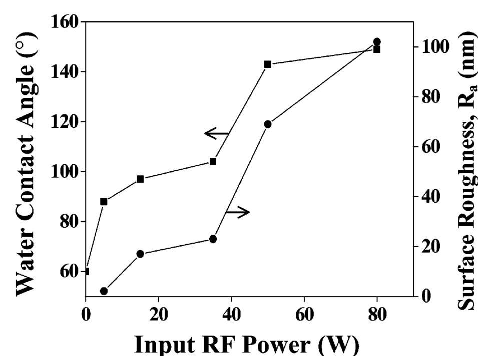

Fig. 5 Effect of the input RF power on the static water contact angle and the surface roughness of the pp-APFB-Cu surfaces.

The roughness factor is therefore equal to 1 for a 'smooth' surface and is always greater than 1 for a real surface. Thus, the hydrophobicity of a surface can be enhanced (*i.e.* becomes even more hydrophobic) by increasing the roughness of the surface appropriately. The same applies to the hydrophilicity of a surface (*i.e.* the surface becomes even more hydrophilic with increasing surface roughness). Thus, the large water contact angle, or the ultra-hydrophobicity, of the pp-APFB-Cu surface prepared at a high RF power has probably resulted from the combined effects of the preservation of the hydrophobic species and the increase in surface roughness. In this case, the minor loss in hydrophobic species due to defluorination is more than compensated by the substantial increase in surface roughness.

3.5 Interaction of the pp-APFB Film with the copper surface

For the application of the pp-APFB film as a reliable dielectric or passivation layer on a copper surface for microelectronic applications, the deposited dielectric layer should exhibit good adhesion with the copper substrate. The interaction between the pp-APFB film and the copper substrate was evaluated by solvent extraction and the Scotch® tape peel test.

Figs. 6(a) and 6(b) show the respective C 1s core-level spectra of the pristine copper foil surface and the 20-s N_2 plasma-pretreated copper foil surface. The C 1s core-level spectra of the pp-APFB films, deposited at a RF power of 5 W, on the corresponding copper foil surfaces are shown in Figs. 6(c) and 6(d). The pp-APFB films on both foil surfaces have been annealed at 260 °C for 1 h, followed by solvent extraction with methyl ethyl ketone. The C 1s core-level spectrum of the pristine copper foil surface consists of four peak components at BEs of 284.6 eV, 286.2 eV, 287.4 eV, and 288.6 eV, attributable to the C–C/C–H species, C–O species, C=O species and O–C=O species, respectively. These species are probably associated with the surface carbon contaminants.[31] Under ambient conditions, surfaces of common metals, such as copper and aluminium, are also covered by hydrated oxides.[32] By comparison of the C 1s spectrum in Fig. 6(a) to that in Fig. 6(c) and that in Fig. 6(d), the removal of the pp-APFB layer from the pristine copper surface by the solvent extraction process is obvious. The N_2 plasma pretreatment of the copper surface is accompanied by the incorporation of nitrogen species onto the copper surface, as indicated by the appearance of the N 1s core-level signal on the copper surface (insert of Fig. 6(b)). The pp-APFB layer is retained to a significant extent on this copper surface after the solvent extraction process. The intensity of the C̲F (aromatic) peak component in Fig. 6(d) decreases slightly after the solvent extraction, in comparison to that prior to the solvent extraction (Fig. 1(a)). The [F]/[C] ratio of the pp-APFB-Cu surface shows a moderate decrease from 0.49 to 0.4 after the solvent extraction. These results indicate that a finite amount of the deposited pp-APFB film has been removed during the solvent extraction process. However, the persistence of the strong intensities for the C̲F (aromatic) peak component and the shake-up satellite in the C 1s spectrum of the pp-APFB layer after the solvent extraction process suggests that the pp-APFB layer is strongly bonded to the N_2 plasma-pretreated copper substrate.

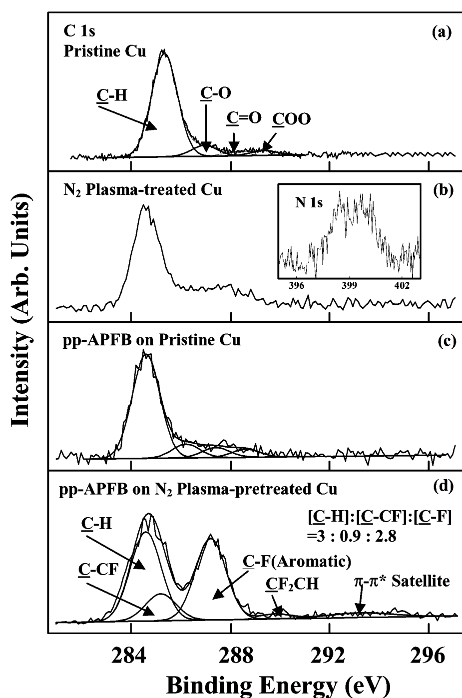

Fig. 6 C 1s core-level spectra of (a) the pristine copper surface, (b) the N_2 plasma-pretreated copper surface, and of the pp-APFB films deposited at a RF power of 5 W on (c) the pristine Cu surface and (d) the N_2 plasma-pretreated Cu surface, after thermal annealing and solvent extraction.

The interaction between the pp-APFB film and the N_2 plasma-pretreated copper substrate was also evaluated by the Scotch® tape peel test. Initially, the pp-APFB-Cu substrate (prepared at a RF power of 5 W) was annealed in a vacuum oven at 260 °C for 1 h and then immersed in methyl ethyl ketone solution for 6 h. The annealing temperature corresponds to the onset of the first major weight loss in the thermogravimetric analysis. Thus, the loosely adhered or bonded pp-APFB chains and oligomers in the pp-APFB film are removed during the thermal annealing process. The annealed and solvent-extracted pp-APFB-Cu surface was adhered to a Scotch® tape. The Scotch® tape was subsequently peeled off from the pp-APFB-Cu surface. The 180°-peel adhesion strength of the Scotch® tape on the pp-APFB-Cu surfaces was in the order of 2 N cm^{-1}. Fig. 7(a) shows the wide scan spectrum of the Scotch® tape surface peeled off from the pp-APFB-Cu substrate. The corresponding spectrum for the delaminated pp-APFB-Cu surface is shown in Fig. 7(b). The presence of fluorine signals in both of the delaminated surfaces and the complete absence of the copper signal on the delaminated copper surface suggest the presence of a predominantly cohesive failure mode inside the pp-APFB layer. The persistence of strong fluorine signals on the delaminated pp-APFB-Cu surface further suggests that the pp-APFB layer is strongly bonded to the N_2 plasma-pretreated copper surface.

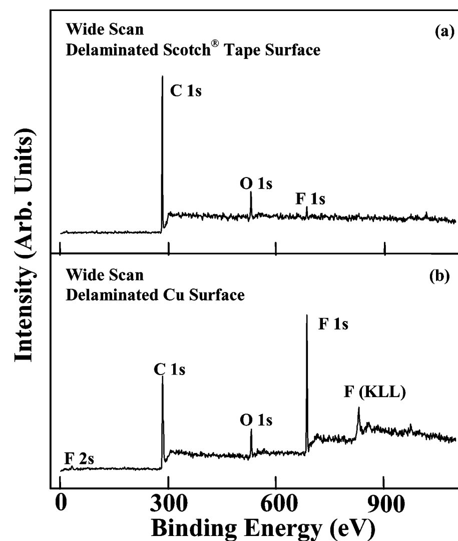

Fig. 7 XPS wide scan spectra of the delaminated (a) Scotch® tape surface and (b) copper foil surface from a Scotch® tape–pp-APFB-Cu assembly, with the pp-APFB film deposited at 5 W.

4. Conclusion

Allylpentafluorobenzene (APFB) was plasma polymerized and deposited on pristine and N_2 plasma-pretreated copper foil surfaces. The effects of the input RF power on surface composition, chemical structure, and morphology of the deposited APFB polymer films were studied by XPS, FTIR, ToF-SIMS, AFM, and SEM. XPS, FTIR and ToF-SIMS results indicated that the fluorinated aromatic ring of the plasma-deposited APFB polymer (pp-APFB) could be retained, to a large extent, under proper glow discharge conditions, such as at a low input RF power. The plasma polymerization of APFB proceeded mainly through the allyl π bonds at low RF power. The preservation of a substantial amount of fluorinated species and the substantial increase in surface roughness for deposition carried out at high RF power (>50 W) gave rise to an ultra-hydrophobic pp-APFB-Cu surface with a static water contact angle as large as 140°. Solvent extraction and Scotch® tape peel test results revealed the presence of strong bonding between the pp-APFB film and the N_2 plasma-pretreated copper foil surface. Thus, plasma polymerization of fluorine-containing monomers provides an alternative approach to the deposition of hydrophobic barriers and passivating thin films on copper surfaces.

References

1 W. W. Lee and P. S. Ho, *MRS Bull.*, 1997, **22**, 19.
2 Y. Shacham-Diamand and V. M. Dubin, *Microelectron. Eng.*, 1997, **33**, 47.
3 S. P. Murarka and S. W. Hymes, *Crit. Rev. Solid State Mater. Sci.*, 1995, **20**, 87.
4 H. Esrom, R. Seebock, M. Charbonnier and M. Romand, *Surf. Coat. Technol.*, 2000, **125**, 19.
5 D. Q. Yang, E. Sacher, E. M. Griswold and G. Smith, *Appl. Surf. Sci.*, 2001, **180**, 200.
6 E. Sacher, *Prog. Surf. Sci.*, 1994, **47**, 273.
7 K. Endo, K. Shinoda and T. Tatsumi, *J. Appl. Phys.*, 1999, **86**, 2739.
8 P. B. Leezenberg, T. C. Reiley and G. W. Tyndall, *J. Vac. Sci. Technol., A*, 1999, **17**, 275.
9 K. Takahashi, A. Itoh, T. Nakamura and K. Tachibana, *Thin Solid Films*, 2000, **374**, 303.
10 S. F. Durrant, S. G. C. Castro, L. E. Bolvar-Marinez, D. S. Galvão and M. A. B. de Moraes, *Thin Solid Films*, 1997, **304**, 149.
11 R. d'Agostino, F. Cramarossa and F. Illuzzi, *J. Appl. Phys.*, 1986, **61**, 2754.
12 H. Yasuda, *Plasma Polymerization*, Academic Press, New York, 1985.
13 L. C. M. Han, R. B. Timmons and W. W. Lee, *J. Vac. Sci. Technol., B*, 2000, **18**, 799.
14 L. C. M. Han, R. B. Timmons, W. W. Lee, Y. Y. Chen and Z. B. Hu, *J. Appl. Phys.*, 1998, **84**, 439.
15 S. R. Coulson, I. S. Woodward, J. P. S. Badyal, S. A. Brewer and C. Willis, *Langmuir*, 2000, **16**, 6287.
16 L. Sandrin, M. S. Silverstein and E. Sacher, *Polymer*, 2001, **42**, 3761.
17 M. S. Silverstein, L. Sandrin and E. Sacher, *Polymer*, 2001, **42**, 4299.
18 L. Zhang, W. S. Chin, W. Huang and J. Q. Wang, *Surf. Interface Anal.*, 1999, **28**, 16.
19 M. R. Baklanov, S. Vanhaelemeersch, H. Bender and K. Maex, *J. Vac. Sci. Technol., B*, 1999, **17**, 372.
20 W. Chen, A. Y. Fadeev, M. C. Hsieh, D. Oner, J. Youngblood and T. J. McCarthy, *Langmuir*, 1999, **15**, 3395.
21 G. H. Yang, E. T. Kang and K. G. Neoh, *J. Polym. Sci., Part A: Polym. Chem.*, 2000, **38**, 3498.
22 Y. Zhang, K. L. Tan, G. H. Yang, X. P. Zou and E. T. Kang, *J. Adhes. Sci. Technol.*, 2000, **14**, 1723.
23 D. T. Clark and W. J. Brennan, *J. Fluorine Chem.*, 1988, **40**, 419.
24 G. E. Muilenberg, *Handbook of X-ray Photoelectron Spectroscopy*, Perkin-Elmer Corporation, Eden Prairie, MN, USA, 1978, p. 38.
25 H. Yasuda and T. Hirotsu, *J. Polym. Sci., Polym. Chem. Ed.*, 1978, **16**, 743.
26 J. E. Huheey, *Inorganic Chemistry*, 2nd Edition, Harper and Row, New York, Appendix F, 1978.
27 M. Morgen, E. T. Ryan, J. H. Zhao, C. Hu, T. H. Cho and P. S. Ho, *Annu. Rev. Mater. Sci.*, 2000, **30**, 645.
28 C. J. Pouchert, *The Aldrich Library of FT-IR Spectra, Ed. I*, Aldrich Chem. Co. Milwaukee, WI, USA, 1985, Vol. 1, p. 1010.
29 M. M. Neil, D. G. Castner and E. R. Fisher, *Langmuir*, 1998, **12**, 1227.
30 R. J. Good, *J. Am. Chem. Soc.*, 1952, **74**, 5041.
31 J. Richer, L. Stolberg and J. Lipkoski, *Langmuir*, 1986, **21**, 630.
32 E. P. Pluedemann (Ed.), *Silane Coupling Agents*, Plenum, New York, 1991.